J Biomol NMR (2007) 39:187–196
DOI 10.1007/s10858-007-9186-2

ARTICLE

Complexity of aromatic ring-flip motions in proteins: Y97 ring dynamics in cytochrome *c* observed by cross-relaxation suppressed exchange NMR spectroscopy

D. Krishna Rao · Abani K. Bhuyan

Received: 9 June 2007 / Accepted: 8 August 2007 / Published online: 11 September 2007

Abstract Dynamics of large-amplitude conformational motions in proteins are complex and less understood, although these processes are intimately associated with structure, folding, stability, and function of proteins. Here, we use a large set of spectra obtained by cross-relaxation suppressed exchange NMR spectroscopy (EXSY) to study the 180° flipping motion of the Y97 ring of horse ferricytochrome *c* as a function of near-physiological temperature in the 288–308 K range. With rising temperature, the ring-flip rate constant makes a continuous transition from Arrhenius to anti-Arrhenius behavior through a narrow Arrhenius-like zone. This behavior is seen not only for the native state of the protein, but also for native-like states generated by adding subdenaturing amounts of guanidine deuterochloride (GdnDCl). Moderately destabilizing concentrations of the denaturant (1.5 M GdnDCl) completely removes the Arrhenius-like feature from the temperature window employed. The Arrhenius to anti-Arrhenius transition can be explained by the heat capacity model where temperature strengthens ground state interactions, perhaps hydrophobic in nature. The effect of the denaturant may appear to arise from direct protein-denaturant interactions that are structure-stabilizing under subdenaturing conditions. The temperature distribution of rate constants under different stability conditions also suggests that the prefactor in Arrhenius-like relations is temperature dependent. Although the use of the transition state theory (TST) offers several challenges associated with data interpretation, the present results and a consideration of others published earlier provide evidence for complexity of ring-flip dynamics in proteins.

Keywords Arrhenius and non-Arrhenius behavior · Cytochrome *c* · Exchange spectroscopy · Protein dynamics · Ring-flip motion

Abbreviations

EXSY	Cross-relaxation suppressed exchange NMR spectroscopy
GdnDCl	Guanidinium deuterochloride
cyt	Cytochrome
ferricyt	Ferricytochrome

Introduction

In recent years, structural studies by X-ray techniques (Pellicena and Kuriyan 2006) and NMR spectroscopy (Grishaev et al. 2005; Stangler et al. 2006), and mutational analyses (Dill and Shortle 1991; Shaw and Valentine 2007) have greatly facilitated relating structure, conformational changes, function, and stability of proteins. Investigations of protein dynamics are still in its infancy though (Fenimore et al. 2004). Internal dynamics that include small amplitude collective motions (Karplus 1986) and large amplitude cooperative breathing modes (Englander et al. 1972), and other structural fluctuations and deformations at the subglobal level (Ansari et al. 1985) are relatively less understood. The complexity of certain of these processes has been recognized for quite some time in both experimental (Fenimore et al. 2004; Austin et al. 1975; Steinbach

D. Krishna Rao · A. K. Bhuyan (✉)
School of Chemistry, University of Hyderabad, Hyderabad 500046, India
e-mail: akbsc@uohyd.ernet.in

A. K. Bhuyan
School of Life Sciences, University of Hyderabad, Hyderabad 500046, India

et al. 1991) and theoretical studies (McCammon et al. 1979; Karplus 2000). For analytical solutions of experimental data, they often appear complex because of either unusual time evolution or complex temperature dependence or both. In theoretical studies, the complexity surfaces when a suitable reaction coordinate and an appropriate transition state along the coordinate is difficult to define. There, of course, is the problem of current atomistic simulations not reaching times longer than microseconds. However, a comprehensive description of protein motions is important not only for connecting structure and function to dynamics, but also for understanding their role in folding and stability of native and natively unfolded states (Portman et al. 2001; Okazaki et al. 2006; Doan-Nguyen and Loria 2007).

This paper presents the temperature and denaturant-related complexity of the ring motion of Y97 side chain (180° rotational jump of the ring about the C_β–C_γ bond axis) of horse ferricytochrome *c* observed by cross-relaxation suppressed exchange NMR spectroscopy (EXSY). The rate of the process does not follow Arrhenius temperature dependence under native and native-like conditions. The changes in the rate-temperature trend under different conditions of protein stability appear to indicate temperature dependence of the Arrhenius-type prefactor. Data are analyzed invoking a heat capacity model that assumes a considerable change in the ground-state heat capacity with temperature.

Starting with the seminal work of Wüthrich and Wagner (1975) on BPTI, the rate-temperature relationship for aromatic ring flip has been reported for just about four proteins to date: BPTI (Wagner et al. 1976; Otting et al. 1993; Li et al. 1998; Skalicky et al. 2001), ferrocytochrome *c* (Campbell et al. 1976), iso-2-cytochrome *c* (Nall and Zuniga 1990), and HPr protein (Hattori et al. 2004). Although the activation parameters from all data sets, generated largely by simulation of variable temperature NMR spectra, were extracted by assuming temperature independence of enthalpy and entropy in the Eyring equation, we believe they are generally temperature dependent to different extents, and hence could be modeled better by using temperature dependent functions. Indeed, this was indirectly observed in a revisit to the BPTI Y35 ring-flip dynamics (Otting et al. 1993). Also, rate-temperature curves calculated for several cases (Skalicky et al. 2001) using activation parameters published earlier indicate visibly non-Arrhenius behavior. Together with the observations of the present study of ferricytochrome *c*, ring-flip dynamics appear generally complex.

Materials and methods

All experiments were performed using cytochrome *c* (Type VI from Sigma) and GdnHCl (from USB, GE Healthcare) the labile hydrogens of both of which were preexchanged for deuterium. Exposure of D_2O solutions of cytochrome *c* to pH 10 at 60°C for an hour followed by lyophilization of the neutralized solution caused complete deuteration of the labile proton sites. GdnDCl was prepared by repeated lyophilization of D_2O solutions of the denaturant.

NMR spectroscopy

A 2-mM solution of cytochrome *c* containing a desired concentration of GdnDCl was prepared in 50 mM phosphate buffer in D_2O, pH 6.5. The same sample was used to take variable-temperature NOESY and EXSY spectra. Each 2D spectrum was of $400t_1$ increments and $2048t_2$ data points over a spectral width of 18 ppm. Quadrature detection along the indirectly detected dimension was achieved by the States-TPPI method. For exchange rate measurement at a given concentration of GdnDCl and temperature, EXSY spectra (Fejzo et al. 1991) were recorded using five mixing times (10, 20, 30, 40, and 50 ms). The details of the mixing pulse scheme are shown in Fig. 1. With 128 scans averaged for each t_1, the time required for a 2D spectrum was over 16 h at 400 MHz. Spectra were recorded using a Bruker spectrometer, and processed and analyzed with XWIN NMR (Bruker) and Felix (Accylrysis) softwares.

Results and discussion

Y97 ring-flip rate constant as a function of protein stability coordinate measured by NMR spectroscopy

The earliest NMR investigations of protein dynamics that employed techniques of 1D time-resolved saturation transfer, isotope-edited spectroscopy in conjunction with spectra simulation, and analysis of temperature dependence of resonances have made several fundamental contributions to the understanding of aromatic ring rotational motions in proteins (Wüthrich and Wagner 1975; Wagner et al. 1976; Skalicky et al. 2001; Nall and Zuniga 1990). The advent of 2D NMR spectroscopy has greatly facilitated studies of such dynamic processes that are too slow to affect the lineshapes (Ernst et al. 1988; Roder 1989). Subsequent introduction of pulse sequences designed to produce chemical exchange cross-peaks by elimination of cross-relaxation and spin coupling-induced coherence transfer effects in 2D spectra (Fejzo et al. 1990, 1991) has further augmented the NMR approach to studies of exchange dynamics in proteins. Indeed, numerous recent work have employed EXSY to investigate dynamic effects; particularly, the ring inversion phenomenon in biology and

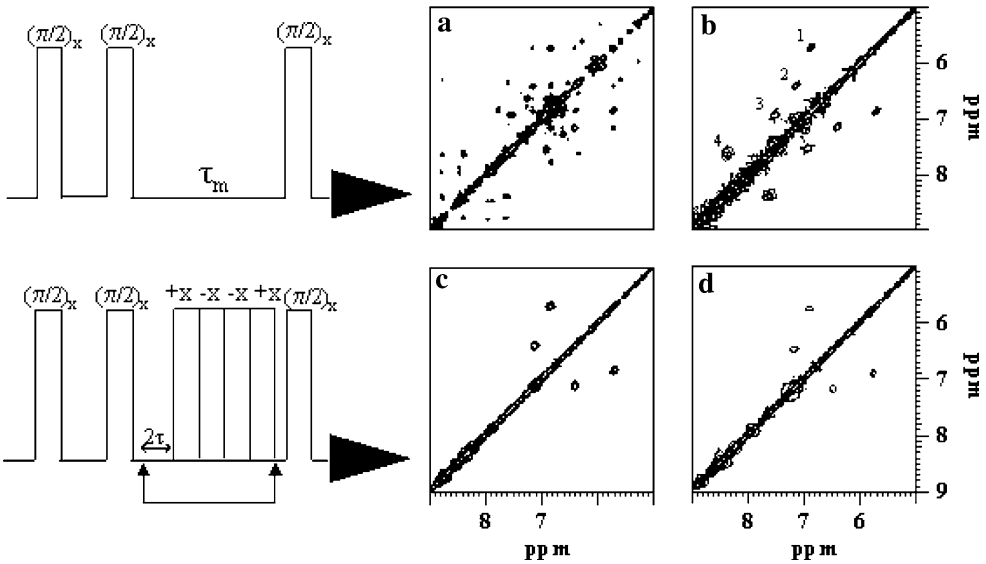

Fig. 1 Relaxation suppressed EXSY largely eliminates NOESY peaks. (**a**) The aromatic region of a NOESY spectrum of ferricyt *c* at 22°C, pH 6.3. The same region of EXSY spectra recorded with the same sample at 20°C (**b**), 30°C (**c**), and 35°C (**d**). Cross peak labels in (**b**) are 1: $Y97_{3,5}$; 2: $Y97_{2,6}$; 3: $F10_{2,6}$; and 4: $F10_{3,5}$. The pulse sequences shown at the left are for NOESY (*top*) and EXSY (*bottom*)

chemistry (Skalicky et al. 2001; Shokhirev et al. 1997; Whittaker et al. 1998; Lam and Carlier 2005; Gallego 2004).

With the objective of characterizing the NMR-defined slow dynamic processes in cytochrome *c* under native to mild denaturing conditions, we collected a large set of exchange spectra recorded at several low concentrations of GdnDCl, each as a function of temperature, and in turn as a function of mixing time in the 0–50 ms range. This approach allows mapping the activation parameters for the rate processes, as the protein is progressively destabilized. Figure 1 presents excerpts from the data set showing the extraction and temperature dependence of cross peaks due to rotational motions of Y97 and F10 rings in native cytochrome *c*. Another ten cross peaks assigned to P30 $C_\beta H$, L68 $C_\delta H_3$, Y48/T42 $C_\alpha H$, T28 $C_\gamma H$, F36/T47 $C_\beta H$, K22/G23 $C_\alpha H$, C14/Q16 $C_\gamma H$, $F82_{2,6}$, F46 $C_3 H$, and H26 Cβ appear in the aliphatic region of the native-state spectrum at 22°C.

To calculate the rate coefficients and activation parameters of the dynamic processes along the protein stability coordinate, it is necessary that the set of exchange-connected cross peaks in the NMR spectrum consistently appear at all concentrations of the denaturant in a suitable range of temperature. However, since both temperature and denaturant affect the dynamics, those processes the interconversion times of which are shorter or longer than the mixing time of the NMR experiment fail to produce cross peaks; shorter interconversion times lead to exchange broadening, and longer interconversion times make only a minute fraction of exchanging population available for interrogation. Such conditions do not produce quantifiable cross peaks. The requirement of the suitable exchange time severely constrains the number of cross peaks, and hence the dynamic processes that can be examined in detail. Two cross peaks, $Y97_{3,5}$ and $Y97_{2,6}$, (peaks 1 and 2, respectively, in Fig. 1b) corresponding to 180° rotational motion of the Y97 ring are consistently observed in the 288–313 K temperature range at 0–1.5 M GdnDCl concentration, and were used for further analysis. The ring-flipping rate constant, k_{flip}, was calculated according to Ernst et al. (1988),

$$\ln(-2\Gamma + 1) = -2k_{\text{flip}}\tau\text{m}, \tag{1}$$

where $\Gamma = V_c/(V_c + V_d)$ with V_d and V_c the diagonal and cross-peak volumes, respectively, and τ_m is the mixing time. Figure 2 shows an example of the plot of $\ln(-2\Gamma + 1)$ versus τ_m.

Values of k_{flip} thus obtained should preferably be corrected for the viscosity effect due to GdnDCl. Although the relative viscosity of the medium increases only marginally in the range of denaturant concentrations used in this study (0–1.5 M), a correction can be introduced according to $k_{\text{flip}} \propto 1/\eta$, where η is the bulk viscosity. To eliminate the effect of viscosity due to GdnDCl on the ring-flip rate constant, we simply use relative viscosity η/η_o, where η_o is the viscosity in the absence of GdnDCl. The corrected k_{flip} (Table 1) is then given by the relation

$$\ln k_{\text{flip}}^{\text{corr}} = \ln k_{\text{flip}} + \ln\left(\frac{\eta}{\eta_o}\right). \tag{2}$$

To obtain the values of η/η_o, we used viscosity of aqueous solutions of GdnDCl from literature (Kawahara and Tanford 1966), and found the following empirical relation

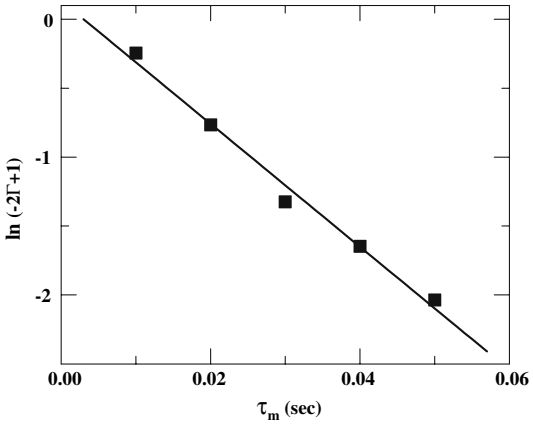

Fig. 2 Extraction of the flip rate constant for the Y97 ring in the native protein at 20°C, pH 6.3. The experimental procedure and data analyses are detailed in the text

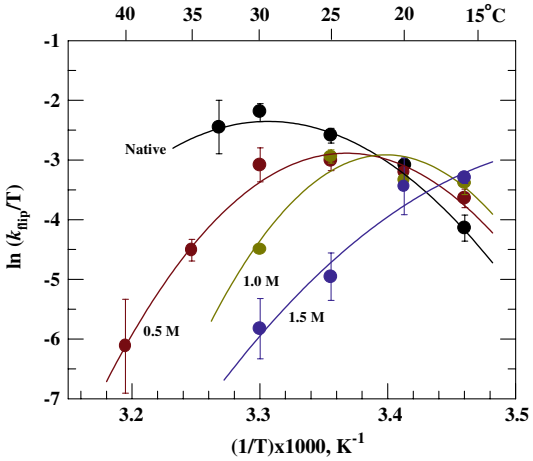

Fig. 3 Temperature dependence of the Y97 ring-flip rate constant at four concentrations of GdnDCl: 0 M (*black*), 0.5 M (*red*), 1.0 M (*yellow*), and 1.5 M (*blue*). Solid lines are fits to data by equation 6. Values of $\Delta H^{\ddagger}$, $\Delta C_p^{\ddagger}$, and $\Delta S^{\ddagger}$ obtained from the fits are listed in Table 2

Table 1 Values of k_{flip} (s^{-1}) as a function of temperature and GdnDCl concentration

Temperature (K)	GdnDCl (M)			
	0	0.5	1.0	1.5
289	4.60	7.56	9.47	10.66
293	13.25	11.85	10.41	9.39
298	22.30	14.56	15.75	2.10
303	33.40	13.91	3.36	0.89
306	26.48	–	–	–
308	–	3.38	–	–
313	–	0.68	–	–

Error in determination of rates: 2–20%

$$\frac{\eta}{\eta_o} = 1 + 0.005[D]^{2.6144} + 0.018[D]^{0.6594} + 0.01213[D]^{0.6636}, \quad (3)$$

where $[D]$ represents molar concentration of GdnDCl.

Non-Arrhenius behavior for the ring-flip rate constant

The temperature dependence of k_{flip} for Y97 at four concentrations of GdnDCl is presented in Fig. 3. The plots of $\ln(k_{\text{flip}}/T)$ against $1{,}000/T$ are not at all linear. The gradients for the curves at 0, 0.5, and 1 M GdnDCl make continuous transition from negative at low temperatures to positive at high temperatures, more accentuated for the latter two concentrations of the denaturant. In general, we identify the curved temperature dependence of rate constants with non-Arrhenius behavior, which could be operationally termed Arrhenius-like (negative slope) or anti-Arrhenius (positive slope) for a small segment of the temperature axis. Indeed, one notices a gradual turn from Arrhenius-like to anti-Arrhenius behavior as the temperature is raised from 15 to 40°C. At 1.5 M GdnDCl, where the protein is still native-like but denaturing conditions are approached (Kumar and Bhuyan 2005), the flip rate constant shows only anti-Arrhenius temperature dependence.

To explain the diminishing enthalpic but growing entropic contribution to the ring isomerization barrier with increasing temperature, we chose to use the transition state theory (TST) rate expression. For justification of this choice, a detailed consideration of reaction rate theory more appropriate for protein reactions is required, a general understanding of which is still not available. It is also uncertain if the ring motion is fully in the diffusive regime, so a Kramers-like rate description becomes essential. The magnitude of the internal friction, and the extent of influence of system–solvent collisions on the ring-flip reactive trajectories across the barrier are other uncertainties. Further, the ring motion is unlikely to be associated with a low and flat barrier for which one might expect a diffusive rate. On the other hand, within the limitations of presently available reaction rate theories and microscopic models, a full justification for the adequacy of TST is difficult to achieve. To make progress with the data at hand, we started with the Eyring-type expression

$$\ln k_{\text{flip}} = \ln A - \frac{\Delta G^{\ddagger}}{RT}, \quad (4)$$

where $\Delta G^{\ddagger} = \Delta H^{\ddagger} - T\Delta S^{\ddagger}$ is the barrier free-energy. The exact nature of the prefactor A is not known; it is perhaps determined by microscopic dynamics entailed in barrier crossing (Portman et al. 2001). $\Delta G^{\ddagger}$ is expanded by casting the enthalpy and entropy changes in their basic forms

$$\Delta H_T^{\ddagger} = \Delta H_{T_0}^{\ddagger} + \int_{T_0}^{T} \Delta Cp^{\ddagger}\, \mathrm{d}T \quad \text{and}$$
$$\Delta S_T^{\ddagger} = \Delta S_{T_0}^{\ddagger} + \int_{T_0}^{T} \Delta Cp^{\ddagger} \frac{\mathrm{d}T}{T}, \tag{5}$$

which allow evaluation of enthalpy and entropy changes at temperatures T with respect to a reference temperature T_0. $\Delta C_p^{\ddagger}$ is the difference in heat capacity of the transition state and the initial state. We set T_0 at 25°C (see below), although for accurate calculations of heat-induced conformational transitions, the midpoint temperature should be used. Thus, the equation

$$\ln k_{\mathrm{flip}} = \ln A - \frac{1}{RT}\left[\Delta H_{T_0}^{\ddagger} + \Delta C_p^{\ddagger}(T - T_0) - T\left(\Delta S_{T_0}^{\ddagger} + \Delta C_p^{\ddagger} \ln\left(\frac{T}{T_0}\right)\right)\right] \tag{6}$$

was used to fit the data shown in Fig. 3. Values of $\Delta H^{\ddagger}$, $\Delta S^{\ddagger}$, and $\Delta C_p^{\ddagger}$ for all four curves are listed in Table 2.

Variation of the activation parameters along the protein stability coordinate

The details of the ring-flip activation parameters in the presence of low concentrations of GdnDCl could potentially provide important information regarding collective motion, stability, and interactions of the relevant structural elements under subdenaturing to denaturing conditions. For scaling the activation parameter, it is reasonable to assume that the changes of the differences in thermodynamic properties between the transition state and the ground state under different conditions of temperature and stability are largely due to effects at the ground state level (see Oliveberg et al. 1995), because the state variables are expected to cause relatively less changes in the thermodynamic properties of a changing transition state which is structurally diminished and distorted.

Table 2 Activation parameter for flipping motion of the Y97 ring

GdnDCl (M)	Parameter		
	$\Delta H^{\ddagger}$ (kcal mol^{-1})	$\Delta C_p^{\ddagger}$ (kcal mol^{-1} 1,000 K^{-1})	$\Delta S^{\ddagger}$ (kcal mol^{-1} 1000 K^{-1})
0.0	15.3	–3.448	0.019
0.5	–4.9	–4.697	–0.049
1.0	–25	–6.645	–0.117
1.5	–38	–2.196	–0.165

Estimated error range for these values is 3–5%

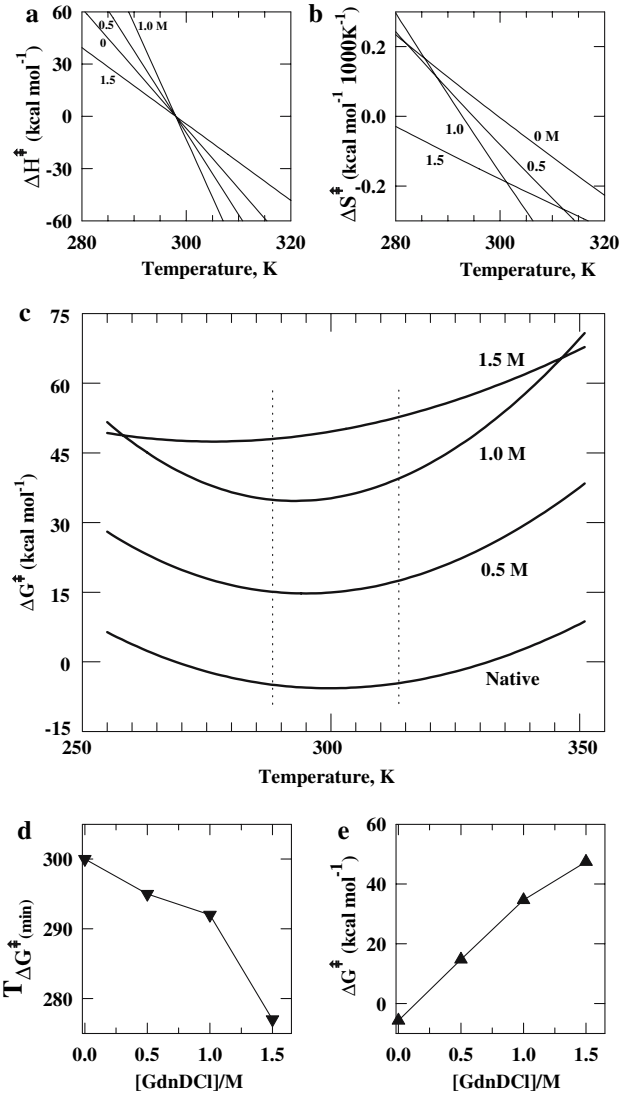

Fig. 4 Thermodynamic parameters for the Y97 ring-flip dynamics calculated from the data shown in Fig. 3. Temperature distribution of (**a**) $\Delta H^{\ddagger}$, (**b**) $\Delta S^{\ddagger}$, and (**c**) $\Delta G^{\ddagger}$ for the four concentrations of GdnDCl indicated. The vertical dotted lines in panel (**c**) show the temperature range used in this study. (**d**) GdnDCl distribution of the temperature corresponding to minimal $\Delta G^{\ddagger}$. (**e**) GdnDCl distribution of the minimal $\Delta G^{\ddagger}$

The temperature gradient of $\Delta H^{\ddagger}$ (Fig. 4a) is negative for all concentrations of GdnDCl. The curves precisely indicate the turn from Arrhenius to anti-Arrhenius through a relatively smaller Arrhenius-like zone of temperature. For all conditions, the value of $\Delta H^{\ddagger}$ passes from positive to negative with increasing temperature registering 'zero' at 298 K, a consequence of choosing T_o = 298 K. Obviously, T_o cannot be 298 K all along the stability coordinate. Even for the native state, the chosen T_o may be way off. It is hard to determine the melting temperature for the specific subglobal part of the protein that is involved in the ring isomerization process. Nonetheless, the arbitrary choice of T_o can still

provide qualitative information and relative values of activation parameters, since the temperature gradient of $\Delta H^{\ddagger}$ will depend little on T_o. The increase in the slope of the enthalpy curves with increments of GdnDCl up to 1 M (Fig. 4a) suggests that in the subdenaturing limit of its concentration, the denaturant acts to increase the difference in heat capacity between the transition state and the ground state ($\Delta C_p^{\ddagger}$). At 1.5 M GdnDCl, denaturing conditions are approached, and $\Delta C_p^{\ddagger}$ begins to shrink. This is also seen from the values listed in Table 2, where the –ve sign for $\Delta C_p^{\ddagger}$ indicates larger values for the ground state C_p. An interpretation of this result could be that within the subdenaturing limit of its concentration, GdnDCl somehow modulates the solvent properties and introduces additional interactions by virtue of its mechanism of action on proteins. This aspect of GdnDCl–protein interaction and the consequences thereof is being discussed in detail in a later section.

Like the temperature dependence of $\Delta H^{\ddagger}$, the value of $\Delta S^{\ddagger}$ passes from positive to negative with increasing temperature for all concentrations of GdnDCl (Fig. 4b). Clearly, the entropic contribution to the barrier energy dominates in the respective anti-Arrhenius temperature zones (Fig. 3). The slope of the entropy–temperature curve increases in going from 0 to 1 M denaturant, suggesting that in the presence of increasing subdenaturing concentrations of GdnDCl, relatively large-scale conformational constraint must be negotiated to make to the transition state. The constraint is generated by the binding interaction of the denaturant with the protein. The decrease of the slope at 1.5 M denaturant is due to the onset of denaturation, where entropy-lowering restraints in the ground state begin to weaken because of increasing structure-breaking action of the denaturant in at least that part of the protein molecule which harbors the flipping ring.

Temperature variation of $\Delta G^{\ddagger}$ for different concentrations of GdnDCl, plotted in Fig. 4c, shows vertical shift of energy and horizontal shift of the temperature corresponding to the energy minimum. The magnitude and the sign of these shifts are specific to the reference temperature chosen (T_o = 298 K). For the same reason, $\Delta G^{\ddagger}$ value for the native-state protein comes out as negative, and therefore, the shifts obtained from Fig. 4c must be scaled relatively. Figure 4d shows how the temperature corresponding to minimal $\Delta G^{\ddagger}$ decreases with increasing amount of GdnDCl; this is due to the general destabilizing action of the denaturant. On the other hand, the increase in the minimal $\Delta G^{\ddagger}$ with denaturant (Fig. 4e), implying a lowering of the free energy of the ground state relative to the transition state, is due to the stabilizing action of the denaturant. The increase is nonlinear though, suggesting that the initial protein stabilization caused by subdenaturing amounts of GdnDCl withers as denaturation begins to set in (see below). By magnitude, the increase of $\Delta G^{\ddagger}$ as a function of GdnDCl is nearly the same within the temperature range employed in our experiment (marked by dotted line in Fig. 4c). The observed variation of rates in this temperature range, however, appears complex. For example, the k_{flip} value for 0 M GdnDCl relative to that for 1 M GdnDCl is an order of magnitude larger at 30°C, is matching at ~20°C, and is smaller at lower temperature. These differences are not due to error of measurement. They rather originate from a temperature dependence of the prefactor A, possibly compounded by the effect of GdnDCl on the internal friction of the protein (see below for a discussion on the internal friction).

Temperature dependence of $\Delta G^{\ddagger}$

In Arrhenius-type rate expressions, $\Delta G^{\ddagger}$ should be virtually independent of temperature. However, variable degrees of temperature dependence of $\Delta G^{\ddagger}$ have been described for different systems, including simple metathesis reactions (Benson and Dobis 1998; Krasnoperov et al. 2006) enzyme mechanisms (Truhlar and Kohen 2001), DNA fluctuations (Wallace et al. 2001), protein–ligand reactions (Austin et al. 1975), and protein refolding kinetics in general (Oliveberg et al. 1995; Chan et al. 1989). The unusual temperature dependence of certain gas-phase reactions has been explained by a modified TST (Krasnoperov et al. 2006). For protein reactions, folding processes in particular, two explanations are provided to account for temperature dependence of $\Delta G^{\ddagger}$. The first, explicable by statistical mechanical principles, is derived for a random walk of an activation within a Gaussian distribution of conformations (Bryngelson and Wolynes 1989), and is often referred to as super-Arrhenius temperature dependence where $\exp -(\Delta G^{\ddagger}/RT)^2$ is used instead of $\exp -(\Delta G^{\ddagger}/RT)$ in the rate-temperature expression (Bryngelson et al. 1995; Scalley and Baker 1997). The second, based on foolproof experimental evidence for strong temperature dependence of hydrophobic interactions (Baldwin 1986; Dill 1990), proposes that temperature dependence of $\Delta G^{\ddagger}$ is due to the disruption of large buried apolar surfaces in going from the ground state to the transition state; the associated heat capacity change $\Delta C_p^{\ddagger}$, and hence $\Delta G^{\ddagger}$, is strongly temperature dependent (Oliveberg et al. 1995; Chan et al. 1989). Another explanation, more appropriate for bimolecular protein reactions, accords complex temperature dependence of $\Delta G^{\ddagger}$ when the binding rate competes with the rates of conformational fluctuations or relaxations of the target site. A well-documented example is rebinding of CO after flash photolysis of carbonmonoxymyoglobin at low temperature (Austin et al. 1975; Steinbach et al. 1991).

Of these, the second explanation corresponds to the heat capacity model used here for analyzing the ring-flip data.

The heat capacity model draws support from strong connections recognized for large amplitude breathing motions of the protein and the ring isomerization event (Wagner et al. 1976; Otting et al. 1993; Skalicky et al. 2001; Hattori et al. 2004; Wagner and Wüthrich 1978). Since deformations of structure and interactions are involved in large amplitude breathing modes (Englander et al. 1972; Englander and Mayne 1992), a difference in heat capacity between the transition state and the ground state ($\Delta C_p^{\ddagger}$) is expected. It is also generally accepted that $\Delta C_p^{\ddagger}$ contributes at least in part to non-Arrhenius temperature dependence of protein reactions. The less preference for the use of a super Arrhenius-type model for ring-flip analysis rests on two considerations. First, unlike the folding of protein chains, ring-flip dynamics is not quite a diffusive process in configurational space. Second, the super-Arrhenius relation applies better for an extended temperature range. At temperatures well above the glass transition, the rate coefficient is smaller than the relation predicts (Steinbach et al. 1991).

Challenges associated with data interpretation

The analyses and discussions presented above also illustrate some of the major difficulties associated with data interpretation and calculation of heat capacity differences between ground and excited states. Fundamentally, the use of a kinetic theory and an Eyring-like expression modeled on simple chemical reaction may not necessarily lead to uncontestable insight. Even when granted, the use of an arbitrarily chosen constant reference temperature (T_o = 298 K) provides at best a qualitative picture, because the value of T_o must change according to the protein stability influenced by the denaturant. Accurate values for T_o relevant for the subglobal part harboring the ring are often difficult to obtain. Another concern is that the ground and excited states vary greatly as a function of denaturant concentration and temperature. Clearly, a detailed knowledge of the landscape topography under denaturing to native-like conditions (i.e., near the bottom of the funnel) is essential for a more quantitative description of the problem. We should mention that the strong temperature dependence of exchange rate of a buried water molecule in BPTI has been previously associated with internal motions involving multiple conformational substate interconversions in a rugged energy landscape (Denisov et al. 1996).

Structural basis for non-Arrhenius ring-flip dynamics in cytochrome *c*

As mentioned already, fairly good evidence exists for the concerted control of large-scale protein motions on the ring isomerization process. Assuming generality of this, numerous influential work on structure and folding of cytochrome *c* facilitates surmising the motional mode that could drive the Y97 ring-flip process. Y97 is a resident of the C-terminal helix, and it is near this residue that the N- and C-terminal helices form a tight contact to produce an orthogonal geometry of helix docking (Fig. 5; see also Roder et al. 1988; Bushnell et al. 1990). This contact region is made of predominantly hydrophobic residues that are highly conserved, and the majority of the very slowly exchanging amide protons, including residues 94–99, are found on the N- and C-terminal helices (Roder et al. 1988). Sufficient exposure of the hydrophobic surface may be required to allow flipping motion of the Y97 ring. We do not have a direct evidence to show how the motion of the helices arranges for the ring-flip. Reports that an early kinetic intermediate of cytochrome *c* comprises the structures of these two helices (Roder et al. 1988; Elöve et al. 1994), the corresponding peptides in solution self-associate (Wu et al. 1993), and that the associated structure of these helices in the native protein forms a low-energy cooperative unfolding unit simulating the global unfolding behavior (Maity et al. 2006), all provide a seeming basis to assume that intrinsic association and dissociation or relative sliding motions of the docked helices render Y97 ring flipping. In thermodynamic terms, the relative motions of the helices that expose the hydrophobic surface in the vicinity of Y97 involve a sizable heat capacity C_p, the magnitude of which increases with strengthening of the hydrophobic interactions by temperature. This motional mechanism must be treated as a possibility. The $\Delta C_p^{\ddagger}$ value is negative for all curves (Table 2), implying that an extensive hydrophobic surface characterizes the ground state, and a large heat is involved in the dissolution of the surface.

Complex action of GdnDCl and temperature on protein stability and ring-flip rate

One of the major objectives of this study was to learn how the rates of slow dynamic processes, Y97 ring-flip in the context, change as the protein is placed in incrementally destabilizing conditions. A gradual decrease of k_{flip} occurs with increments of GdnDCl, clearly noticeable at temperatures higher than ~20°C. This general decrease can be explained by constrained dynamics of the protein as a result of its interaction with the denaturant. An explanation and the illustration of this effect in the case of cytochrome *c* has been provided in two of our earlier papers reporting on a different set of experiments (Bhuyan 2002; Kumar et al. 2004). Briefly, GdnDCl can interact directly with protein backbone and side-chains by variable-length

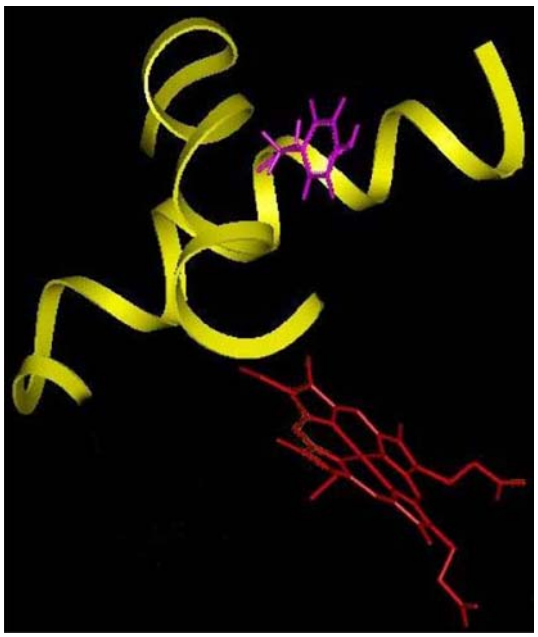

Fig. 5 The N- and C-terminal helices of cytochrome *c* with the disposition of the Y97 ring as seen in the crystal structure (PDB file: 1HRC; Bushnell et al. (1990)). Also shown is the heme ring

hydrogen bonding and van der Waals interactions (Dunbar et al. 1997; Makhatadze and Privalov 1992; Pike and Acharya 1994; Zarrine-Afsar et al. 2006). Such interactions produce cross-links or non-specific network of intraprotein interactions (Dunbar et al. 1997), leading to protein stiffening, reduction of motional freedom, increased internal friction, and thus entropic stabilization. In the present case also, GdnDCl-induced constraints on the motions of N- and C-terminal helices of cytochrome *c* is likely to retard the ring-flip motion. The protein stabilizing effect of subdenaturing amount of GdnDCl is overrun by its structure unfolding action when used at higher concentrations. The present results indicate that the denaturing effect begins to appear at $\sim$1.5 M GdnDCl.

But the observed k_{flip} dependence on GdnDCl is more complex when the temperature variable is brought into picture. The k_{flip}-temperature curves appear to meet near 20°C, and diverge on either side showing a reversal of temperature dependence (Fig. 3), suggesting that the ring flip rate constant near this temperature does not change with GdnDCl as long as the latter is present in subdenaturing concentrations. The slight difference in the behavior of the curve for 1.5 M GdnDCl is likely due to approach of denaturing conditions. This behavior of k_{flip} as a function of denaturant and temperature (Fig. 3) is inconsistent with the temperature distribution of $\Delta G^{\ddagger}$ at the four GdnDCl concentrations (Fig. 4c). The vertical dotted lines in Fig. 4c show the temperature range used in our experiments, and within this range the variation of $\Delta G^{\ddagger}$ with denaturant is very similar for all temperatures, suggesting that the k_{flip} curves for different denaturant concentrations should not converge at any temperature within this range. This observation should mean that the prefactor A is acting in a temperature dependent manner leading to the coalescence of k_{flip} values at $\sim$20°C. But why this happens near 20°C is not clear at present. In Eyring-type relations, A generally shows only weak temperature dependence. However, the fits of the data to the heat capacity model with three floating parameters ($\Delta H^{\ddagger}$, $\Delta C_p^{\ddagger}$, and $\Delta S^{\ddagger}$) cannot rule out a significant nonlinear dependence of A on temperature in a denaturant dependent manner. Studies on the effect of GdnDCl on A in Eyring-type expressions will shed light on this issue.

Aromatic ring-flip motions in other proteins

Following the earliest study with BPTI (Wüthrich and Wagner 1975), ring-flip dynamics of only four proteins, namely, ferrocytochrome *c* (Campbell et al. 1976), fd bacteriophase (Gall et al. 1982), yeast iso-2-cytochrome *c* (Nall and Zuniga 1990), and *S. carnosus* HPr (Hattori et al. 2004) have been studied in some detail, although the problem in BPTI has been revisited on several occasions (Wagner et al. 1976; Otting et al. 1993; Skalicky et al. 2001; Wagner and Wüthrich 1978). In general, the rate strongly varies with packing and dynamics of the ring environment. This is the likely reason why the rates for different aromatic rings within a protein, and for one protein from another could differ, often very significantly, under identical experimental conditions. For example, the rates for Y35 and Y23 of BPTI near room temperature may vary by an order of magnitude, from $\sim 10^2$ to $\sim 10^3$ s^{-1} (Wagner et al. 1976), and the aromatic rings of fd bacteriophage flip at $\sim 10^6$ s^{-1} (Gall et al. 1982).

Even more interesting is the complex temperature dependence, which the present study exposes in some detail. A review of earlier rate-temperature data for ring dynamics in different proteins also reveals some deviation from simple Arrhenius behavior. The temperature dependence of Y35 flip rate constant in BPTI (Wagner et al. 1976), for example, would appear nonlinear unless large errors in data are allowed. As Karplus points out (Karplus 2000), in the reinvestigation of Y35 flip rate by the use of high resolution EXSY, Otting et al. (1993) tie the activation parameters for the flipping process with those for disulfide conformational exchange motion at high temperature. The flip rate at low temperature (<20°C) was not measured. However, since the temperature graph for the activation energy of the disulfide exchange motion shows different dependences at low and high temperatures registering a sharp inflection centered around 20°C, and because

the conformational motion and flip motion are linked, the latter should also follow the trend for the former process and hence a nonlinear function of temperature. In a more recent paper, Skalicky et al. (2001) used activation parameters published earlier to calculate rate-temperature curves for several residues of BPTI, iso-2-cytochrome *c*, and horse cytochrome *c*. The curves in their semilogarithmic plot of k_{flip} versus T, calculated using $1/k_{\text{flip}} = h/(k_{\text{B}}T)\exp[(\Delta H^{\ddagger}/RT - \Delta S^{\ddagger}/R)]$, are clearly not linear. The flip dynamics of Y6 in *S. carnosus* HPr deduced from spectra simulation (Hattori et al. 2004) has been analyzed assuming temperature independence of the activation parameters. Here also, the rate-temperature behavior, especially at 200 Mpa, may not simply be linear; an even closer look is perhaps worth considering. Thus, evidences are rather strong that aromatic ring dynamics in proteins are complex, and they do not follow an Arrhenius-like equation.

Conclusions

Unusual temperature dependence for dynamic processes like ring rotation within a temperature range where spectroscopic measurements do not reveal any change in the time-averaged native structure of the protein is a complex phenomenon by itself. The complexity is compounded when subdenaturing amounts of denaturant act on the protein. Aromatic ring isomerization in dense systems like proteins and polymers involves large amplitude cooperative motion of the ring and certain structural elements, often engaging the chain backbone (Otting et al. 1993; Khare and Paulaitis 1995). We have used the heat capacity model to explain the cytochrome *c* results. Further studies may reveal alternative, perhaps even better models for such phenomena. Irrespective of the merit of the model, the data and evidences presented are compelling that aromatic ring motions are complex.

Acknowledgments This work was supported by grants from the Department of Biotechnology (BRB/15/227/2001), the Department of Science & Technology (4/1/2003-SF), and the University Grants Commission (UPE Funding), Government of India. AKB is the recipient of a Swarnajayanti Fellowship from the DST.

References

Ansari A, Berendzen J, Bowne SF et al (1985) Protein states and proteinquakes. Proc Natl Acad Sci USA 82:5000–5004

Austin RH, Beeson KW, Eisenstein L (1975) Dynamics of ligand binding to myoglobin. Biochemistry 14:5355–5373

Baldwin RL (1986) Temperature dependence of the hydrophobic interaction in protein folding. Proc Natl Acad Sci USA 83: 8069–8072

Benson SW, Dobis O (1998) Existence of negative activation energies in simple bimolecular metathesis reactions and some observations on too fast reactions. J Phys Chem A 102:5175–5181

Bhuyan AK (2002) Protein stabilization by urea and guanidine hydrochloride. Biochemistry 41:13386–13394

Bryngelson JD, Wolynes PG (1989) Intermdeiates and barrier crossing in a random energy model with applications to protein folding. J Phys Chem 93:6902–6915

Bryngelson JD, Onuchic JN, Socci ND, Wolynes PG (1995) Funnels, pathways and the energy landscape of protein folding: a synthesis. Proteins 21:167–195

Bushnell GW, Louie GV, Brayer GD (1990) High-resolution three-dimensional structure of horse heart cytochrome *c*. J Mol Biol 214:585–595

Campbell ID, Dobson CM, Moore GR, Perkins S.J, Williams RJP (1976) Temperature dependent molecular motion of a tyrosine residue of ferrocytochrome *c*. FEBS Lett 70:96–100

Chan B-l, Baase WA, Schellman JA (1989) Low-temperature unfolding of a mutant of phage T4 lysozyme. 2. Kinetic investigations. Biochemistry 28:691–699

Dill KA (1990) Dominant forces in protein folding. Biochemistry 29:7133–7155

Dill KA, Shortle D (1991) Denatured states of proteins. Annu Rev Biochem 60:795–825

Doan-Nguyen V, Loria JP (2007) The effects of cosolutes on protein dynamics: the reversal of denaturant-induced protein fluctuations by trimethylamine N-oxide. Protein Sci 16:20–29

Denisov VP, Peters J, Hörlein HD, Halle B (1996) Using buried water molecules to explore the energy landscape of proteins. Nat Struct Biol 3:505–509

Dunbar J, Yennawar HP, Banerjee S, Luo J et al (1997) The effects of denaturants on protein structure. Protein Sci 6:1272–1733

Elöve GA, Bhuyan AK, Roder H (1994) Kinetic mechanism of cytochrome *c* folding: involvement of the heme and its ligands. Biochemistry 33:6925–6935

Englander SW, Mayne L (1992) Protein folding studied using hydrogen-exchange labeling and two-dimensional NMR. Annu Rev Biophys Biomol Struct 21:243–265

Englander SW, Downer NW, Teitelbaum H (1972) Hydrogen exchange. Annu Rev Biochem 41:903–924

Ernst RR, Bodenhausen G, Wokaun A (1988) Principles of nuclear magnetic resonance in one and two dimensions. Clarendon Press, Oxford

Fejzo J, Zolnai Z, Macura S, Markley JL (1990) Quantitative evaluation of two-dimensional cross-relaxation NMR spectra of proteins. Interprotein distances in turkey ovomucoid third domain. J Magn Reson 88:93–110

Fejzo J, Westler WM, Macura S, Markley JL (1991) Strategies for eliminating unwanted cross-relaxation and coherence-transfer effects from two-dimensional chemical exchange spectra. J Magn Reson 92:20–29

Fenimore PW, Frauenfelder H, McMahon BH, Young RD (2004) Bulk-solvent and hydration-shell fluctuations, similar to alpha- and beta-fluctuations in glass, control protein motions and fluctuations. Proc Natl Acad Sci USA 101:14408–14413

Gall CM, Cross TA, DiVerdi JA, Opella SJ (1982) Protein dynamics by solid state NMR: aromatic rings of the coat protein in fd bateriophage. Proc Natl Acad Sci USA 79:101–105

Gallego J (2004) Sequence-dependent nucleotide dynamics revealed by intercalated ring rotation in DNA-bisnaphthalimide complexes. Nucleic Acid Res 32:3607–3614

Grishaev A, Wu J, Trewhella J, Bax A (2005) Refinement of multidomain protein structures by combination of solution small-angle X-ray scattering and NMR data. J Am Chem Soc 127:16621–16628

Hattori M, Li H, Yamada H, Akasaka K et al (2004) Infrequent cavity-forming fluctuations in HPr from Staphylococcus carnosus revealed by pressure- and temperature-dependent tyrosine ring flips. Protein Sci 13:3104–3114

Karplus M (1986) Internal dynamics of proteins. Methods Enzymol 131:283–307

Karplus M (2000) Aspects of protein reaction dynamics: deviations from simple behavior. J Phys Chem B 104:11–27

Kawahara K, Tanford C (1966) Viscosity and density of aqueous solutions of urea and guanidine hydrochloride. J Biol Chem 241:3228–3232

Khare R, Paulaitis ME (1995) A study of cooperative phenyl ring flip motions in glassy polystyrene by molecular simulations. Macromolecules 28:4495–4504

Krasnoperov LN, Peng J, Marshall P (2006) Modified transition state theory and negative apparent activation energies of simple metathesis reactions: application to the reaction $CH_3 + HBr \rightarrow CH_4 + Br$. J Phys Chem A 110:3110–3120

Kumar R, Bhuyan AK (2005) Two-state folding of horse ferrocytochrome c: analyses of linear free energy relationship, chevron curvature, and stopped-flow burst relaxation kinetics. Biochemistry 44:3024–3033

Kumar R, Prabhu NP, Yadaiah M, Bhuyan AK (2004) Protein stiffening and entropic stabilization in the subdenaturing limit of guanidine hydrochloride. Biophys J 87:2656–2662

Lam PC-H, Carlier PR (2005) Experimental and computational studies of ring inversion of 1,4-benzodiazepin-2-ones: implications for memory of chirality transformations. J Org Chem 70:1530–1538

Li H, Yamada H, Akasaka K (1998) Effect of pressure on individual hydrogen bonds in proteins. Basic pancreatic trypsin inhibitor. Biochemistry 37:1167–1173

Maity H, Rumbley JN, Englander SW (2006) Functional role of a protein foldon- an omega-loop foldon controls the alkaline transition in ferricytochrome *c*. Proteins 63:349–355

Makhatadze GI, Privalov PL (1992) Protein interactions with urea and guanidinium chloride. A calorimetric study. J Mol Biol 226: 491–505

McCammon JA, Wolynes PG, Karplus M (1979) Picosecond dynamics of tyrosine side chains in proteins. Biochemistry 18:927–942

Nall BT, Zuniga EH (1990) Rates and energetics of tyrosine ring flips in yeast iso-2-cytochrome *c*. Biochemistry 29:7576–7584

Okazaki K-i, Koga N, Takada S, Onuchic JN et al (2006) Multiple-basin energy landscapes for large-amplitude conformational motions of proteins: structure-based molecular dynamics simulations. Proc Natl Acad Sci USA 103:11844–11849

Oliveberg M, Tan Y-J, Fersht AR (1995) Negative activation enthalpies in the kinetics of protein folding. Proc Natl Acad Sci USA 92:8926–8929

Otting G, Liepinsh E, Wüthrich K (1993) Disulfide bond isomerization in BPTI and BPTI(G36S): an NMR study of correlated mobility in proteins. Biochemistry 32:3571–3582

Pellicena P, Kuriyan J (2006) Protein–protein interactions in the allosteric regulation of protein kinase. Curr Opin Struct Biol 16:702–709

Pike ACW, Acharya R (1994) A structural basis for the interaction of urea with lysozyme. Protein Sci 3:706–710

Portman JJ, Takada S, Wolynes PG (2001) Microscopic theory of protein folding rates. II. Local reaction coordinates and chain dynamics. J Chem Phys 114:5082–5096

Roder H (1989) Structural characterization of protein folding intermediates by proton magnetic resonance and hydrogen exchange. Methods Enzymol 176:446–473

Roder H, Elöve GA, Englander SW (1988) Structural characterization of folding intermediates in cytochrome *c* by H-exchange labeling and proton NMR. Nature 335:700–704

Scalley ML, Baker D (1997) Protein folding kinetics exhibit an Arrhenius temperature dependence when corrected for the temperature dependence of protein stability. Proc Natl Acad Sci USA 94:10636–10640

Shaw BF, Valentine JS (2007) How do ALS-associated mutations in superoxide dismutase 1 promote aggregation of the protein. Trends Biochem Sci 32:78–85

Shokhirev NV, Shokhireva TK, Polam JR, Watson CT et al (1997) 2D NMR investigations of the rotation of axial ligands in six-coordinate low-spin iron(III) and cobalt(III) tetraphenylporphyrinates having 2,6-disubstituted phenyl rings: quantitation of rate constants from ^{1}H EXSY cross-peak intensities. J Phys Chem A 101:2778–2786

Skalicky JJ, Mills JL, Sharma S, Szyperski T (2001) Aromatic ring-flipping in supercooled water: implications for NMR-based structural biology of proteins. J Am Chem Soc 123:388–397

Stangler T, Hartmann R, Willbold D, Koenig BW (2006) Modern high resolution NMR for the study of structure, dynamics and interactions of biological macromolecules. Z Phys Chem 220:567–613

Steinbach PJ, Ansari A, Berendzen J et al (1991) Ligand binding to heme protein: connection between dynamics and function. Biochemistry 30:3988–4001

Truhlar DG, Kohen A (2001) Convex Arrhenius plots and their interpretation. Proc Natl Acad Sci USA 98:848–851

Wagner G, DeMarco A, Wüthrich K (1976) Dynamics of the aromatic amino acid residues in the globular conformation of the basic pancreatic trypsin inhibitor (BPTI). Biohys Struct Mechanism 2:139–158

Wagner G, Wüthrich K (1978) Dynamic model of globular protein conformations based on NMR studies in solution. Nature 275:247–248

Wallace MI, Ying L, Balasubramanian S, Klenerman D (2001) Non-Arrhenius kinetics for the loop closure of a DNA hairpin. Proc Natl Acad Sci USA 98:5584–5589

Whittaker SB-M, Boetzel R, MacDonald C, Lian L-Y et al (1998) NMR detection of slow conformational dynamics in an endonuclease toxin. J Biomol NMR 12:145–159

Wu LC, Laub PB, Elöve GA, Carey J et al (1993) A noncovalent peptide complex as a model for an early folding intermediate of cytochrome *c*. Biochemistry 32:10271–19276

Wüthrich K, Wagner G (1975) NMR investigations of the dynamics of the aromatic amino acid residues in the basic pancreatic trypsin inhibitor. FEBS Lett 50:265–268

Zarrine-Afsar A, Mittermaier A, Kay LE, Davidson AR (2006) Protein stabilization by specific binding of guanidinium to a functional arginine-binding surface on an SH_3 domain. Protein Sci 15:162–170